Results in Physics 7 (2017) 2607–2613

Contents lists available at ScienceDirect

Results in Physics

journal homepage: www.journals.elsevier.com/results-in-physics

Chemically reactive species in the flow of a Maxwell fluid

Sohail Nadeem [a], Shafiq Ahmad [a,*], Noor Muhammad [a], M.T. Mustafa [b]

[a] Department of Mathematics, Quaid-I-Azam University 45320, Islamabad 44000, Pakistan
[b] Department of Mathematics, Statistics and Physics, Qatar University, Doha 2713, Qatar

ARTICLE INFO

Article history:
Received 9 April 2017
Received in revised form 19 May 2017
Accepted 12 June 2017
Available online 19 June 2017

Keywords:
Cattaneo–Christov heat model
Maxwell fluid
Thermal stratification
Homogeneous and heterogeneous reaction

ABSTRACT

This article presents a research for boundary layer flow and heat transfer of a Maxwell fluid over an exponential stretching surface with thermal stratifications. The effect of homogeneous and heterogeneous reaction are incorporated. Cattaneo–Christov heat flux model is used instead of Fourier law of heat conduction, which is recently proposed by Christov. This model predicts the impacts of thermal relaxation time on boundary layer. The transformed boundary layer equations are solved analytically by using Optimal homotopy analysis method. The effect of non-dimensional fluid relaxation time, thermal relaxation time, Prandtl number, Schmidt number and strength of homogeneous and heterogeneous reaction are demonstrated and exhibited graphically. The comparison of Cattaneo–Christov heat flux model and the Fourier's law of heat conduction is also displayed.

Introduction

In recent years, the analysis of flow and heat transfer over a stretching surface have achieved extensive attention because of its wide applications, such as continuous casting, exchangers, metal spinning, bundle wrapping, foodstuff processing, chemical processing, equipment and polymer extrusion. Crane [1] was the first who study the Newtonian fluid flow caused by a stretching sheet. Many researchers Dutta et al. [2], Chen and Char [3] and Gupta [4] modified the work of Crane [1] by taking the effect of mass transfer under various circumstances. Nadeem et al. [5] took the exponential stretching sheet to discuss the heat transfer phenomenon of water-based nanofluid. Mukhopadhyay et al. [6] scrutinized the heat transfer flow over a porous exponential stretching sheet with thermal radiation. Zhang et al. [7] concentrates the heat transfer of the power law nanofluid thin film occur due to a stretching sheet in the presence of velocity slip effect and magnetic field. The boundary layer flow of ferromagnetic fluid over a stretching surface is demonstrated by Majeed et al. [8]. Pal and Saha [9] examined the unsteady stretching sheet to discuss the heat and mass transfer in a thin liquid film with the effect of non linear thermal radiation. Weidman [10] studied a unified formulation for stagnation point flows with stretching surfaces.

The natural phenomenon of heat transport is widespread in nature as long as there is a temperature difference between object or between various parts of a similar object, there will be phenomenon of heat transfer. In this manner, a significant consideration has been committed to anticipate the heat transfer effect. Therefore Fourier's [11] initiated his famous law known as "Fourier's law of heat conduction". The characteristics of heat transport phenomenon are not completely interpreted by this law. Because no such body exist in nature which obeys Fourier's law of heat conduction. To remove this drawbacks Cattaneo [12] modified flow of heat conduction by adding a relaxation time. Christov [13] employed [12] to the upper convected Maxwell fluid. Cattaneo–Christov heat flux model, states that the heat transferred slowly in a medium and its gives a hyperbolic form of equation. Muhammad and Nadeem [14] analyzed the viscous fluid flow embedded with porous medium past a stretching sheet with Cattaneo–Christov heat flux model and thermal stratification. Hashim [15] considered a stagnation point flow of a Carreau fluid with the effect of Cattaneo–Christov heat flux model over a slandering sheet. Abbas et al. [16] got the analytical solution for the flow of Maxwell fluid over a stretching surface in the presence of Cattaneo–Christov heat flux model. Ramzan et al. [17] used Cattaneo–Christov heat flux model for Maxwell fluid flow over a bidirectional stretched sheet with homogeneous and heterogeneous reaction and magnetohydrodynamic. khan and khan [18] explored the heat transfer and boundary layer flow characteristic to burgers fluid using Cattaneo–Christov heat flux model. Muhammad et al. [19] used Cattaneo–Christov heat flux model to described squeezed flow of a nanofluid in the presence of double stratification.

In the last few decade, the dynamics of non-Newtonian fluids got extensive interest among the scientist. Newtonian's law of viscosity is unable to explain such types of fluids. Many liquids such

* Corresponding author.
E-mail address: ashafiq@math.qau.edu.pk (S. Ahmad).

http://dx.doi.org/10.1016/j.rinp.2017.06.017
2211-3797/© 2017 The Authors. Published by Elsevier B.V.

as soaps, mud, apple sauce, polymer melts, suspension solutions, lubricants, ketchup, oils and many others depicts the rheological characteristics and thus can not be characterized by one constitutive expression. Therefore, non-Newtonian fluid is classified into three sub classes, i.e. integral, differential and rate types. Maxwell fluid belongs to the rate type fluids illustrating the relaxation time effects. Fetecau and Jamil [20] in a current review reported an examination for the helical flows of Maxwell fluid. The Maxwell fluid embedded in a porous layer to for the onset of triple-diffusive convection with internal heat source have been demonstrated by Awasthi et al. [21]. The study of stagnation point flow with Maxwell nanofluid past a permeable stretching sheet is analyzed by Ramesh et al. [22]. Zhao et al. [23] demonstrates the heat transfer analysis of Maxwell fluid via a vertical plate. Li et al. [24] exhibits the heat transfer and coupled flow with generalized fractional Maxwell fluid saturated in a porous medium between two infinite parallel plates. Further applications relevant to heat transport phenomenon may be found in [28–39].

The aim of present work is to analyze the impacts of heat transport phenomenon in a Maxwell fluid in the presence of thermal stratification. The flow is induced by stretching of surface. Cattaneo–Christov heat flux is characterized instead of Fourier's law of heat conduction in the evaluation of heat transfer rate. Further, the effect of chemical reaction is taken into account. The boundary value problem are solved analytically via Optimal HAM. The graphical behavior of emerging parameters are presented.

Mathematical formulation

Consider the steady two dimensional, electrically non-conducting and an incompressible Maxwell fluid over an exponentially stretching surface. The effect of homogeneous and heterogeneous reaction and thermal stratification are incorporated. The movement of the fluid is caused by the exponential stretched surface. The effects of generation/absorption and viscous dissipation are neglected. At $y = 0$ the flow is characterized and the plate is stretched along x-axis with velocity $U_w = U_0 exp(x/l)$. The effect of the chemical reaction are examined in flow analysis. The simple model for the relationship between a heterogenous (or surface) reaction and a heterogeneous (or bulk) reaction including the two chemical species A and B in a boundary layer flow suggested by Merkin and Chudhary [25,26] and Merkin [27] are described as

$$A + 2B \rightarrow 3B, \quad \text{rate} = k_c ab^2 \tag{1}$$

$$A \rightarrow B, \quad \text{rate} = k_s a. \tag{2}$$

In above equations concentration of chemical species A and B are denoted by a and b and $k_i, (i = c, s)$ are the rate constants. Both reaction processes are assumed to be isothermal. Under the boundary layer approximation the continuity, momentum and concentration equations lead to be

$$\frac{\partial u}{\partial x} + \frac{\partial v}{\partial y} = 0, \tag{3}$$

$$u\frac{\partial u}{\partial x} + v\frac{\partial u}{\partial y} + \lambda_1\left(u^2\frac{\partial^2 u}{\partial x^2} + v^2\frac{\partial^2 u}{\partial y^2} + 2uv\frac{\partial^2 u}{\partial x \partial y}\right) = \frac{\mu}{\rho}\frac{\partial^2 u}{\partial y^2}, \tag{4}$$

$$u\frac{\partial T}{\partial x} + v\frac{\partial T}{\partial y} + \lambda_2\Omega_E = \alpha\frac{\partial^2 T}{\partial y^2}, \tag{5}$$

$$u\frac{\partial a}{\partial x} + v\frac{\partial a}{\partial y} = D_A\frac{\partial^2 a}{\partial y^2} - k_c ab^2, \tag{6}$$

$$u\frac{\partial b}{\partial x} + v\frac{\partial b}{\partial y} = D_B\frac{\partial^2 b}{\partial y^2} + k_c ab^2. \tag{7}$$

Here x and y are the respective Cartesian coordinates taken along the surface and perpendicular to it, u and v are the respective velocity components, λ_1 indicate fluid relaxation time, υ is the kinematic viscosity, T express the local fluid temperature, λ_2 demonstrate the relaxation time for heat flux and D_A and D_B are the respective diffusion coefficients.

In above equation the term Ω_E is define as

$$\Omega_E = u\frac{\partial u}{\partial x}\frac{\partial T}{\partial x} + v\frac{\partial v}{\partial y}\frac{\partial T}{\partial y} + u^2\frac{\partial^2 T}{\partial x^2} + v^2\frac{\partial^2 T}{\partial y^2} + 2uv\frac{\partial^2 T}{\partial x \partial y} + u\frac{\partial v}{\partial x}\frac{\partial T}{\partial y} + v\frac{\partial u}{\partial y}\frac{\partial T}{\partial x}. \tag{8}$$

The boundary conditions are of the form

$$\begin{gathered} u|_{y=0} = U_w(x) = U_0\exp(x/l),\ v|_{y=0} = 0,\ T|_{y=0} = T_w = T_\infty + d_1\exp(x/2l), \\ D_A\frac{\partial a}{\partial y}\Big|_{y\to 0} = k_s a(0),\ D_B\frac{\partial b}{\partial y}\Big|_{y\to 0} = -k_s a(0) \\ u|_{y\to\infty} \to 0,\ T|_{y\to\infty} \to T_\infty,\ a|_{y\to\infty} \to a_0,\ b|_{y\to\infty} \to 0, \end{gathered} \tag{9}$$

in the above equation, U_w is the variable stretching velocity, U_0 is the reference velocity and T_∞ exemplify temperature of ambient fluid.

Solution procedure

We institute the stream function ψ where $u = \frac{\partial \psi}{\partial y}$ and $v = -\frac{\partial \psi}{\partial x}$, which fulfills the continuity equation indistinguishably, utilizing similarity transformation of the following form,

$$\begin{gathered} \psi = \exp(x/2l)\sqrt{2\nu l U_0} f(\eta), \quad \eta = y\sqrt{\frac{U_0}{2\nu l}}\exp(x/2l), \\ \theta(\eta) = \frac{T - T_\infty}{T_w - T_\infty}, \quad g(\eta) = \frac{a}{a_0}, \quad h(\eta) = \frac{b}{a_0} \\ u = U_0\exp(x/l) f'(\eta), \quad v = -\sqrt{\frac{\nu U_0}{2l}}\exp(x/2l)\{f(\eta) + \eta f'(\eta)\}. \end{gathered} \tag{10}$$

Here $\theta(\eta)$ signify the unitless temperature and prime symbolize differentiation with respect to η. The fundamental Eqs. (3) to (8) with boundary condition (9) are reduce to ordinary differential equations after applying the similarity transformation (10) i.e.

$$f''' - 2f' + ff'' + \delta m\left(3ff'f'' - \frac{1}{2}f^2 f''' + \frac{1}{2}\eta f'^2 f'' - 2f'^3\right) = 0, \tag{11}$$

$$\theta'' + \mathrm{Pr} f\theta' - \frac{1}{2}\mathrm{Pr}\delta e\left(f^2\theta'' + ff'\theta'\right) = 0, \tag{12}$$

$$\frac{1}{S_c}g'' + fg' - k_1 gh^2 = 0, \tag{13}$$

$$\frac{\delta}{S_c}h'' + fh' + k_1 gh^2 = 0, \tag{14}$$

$$\begin{gathered} f(\eta) = 0, \quad f'(\eta) = 1, \quad \theta(\eta) = 1 - S_1, \quad g'(\eta) \\ = k_2 g(\eta), \quad \delta h'(\eta) = -k_2 g(\eta), \quad \eta = 0, \end{gathered} \tag{15}$$

$$f'(\eta) = 0, \quad \theta(\eta) = 0, \quad g(\eta) = 1, \quad h(\eta) = 0, \quad \eta \to \infty. \tag{16}$$

Here δm is the fluid relaxation time, δe indicate the thermal relaxation time, Pr demonstrate the Prandtl number, S_c is the Schmidt number, S_1 is the thermal stratified parameter, k_1 and k_2 are respectively the strength of homogeneous and heterogeneous reaction and δ is the ratio of diffusion coefficient, and are defined as

$$\delta m = \frac{\lambda_1 U_0}{l}, \quad \Pr = \frac{\nu}{a}, \quad \delta e = \frac{\lambda_2 U_0}{l}, \quad S_c = \frac{\nu}{D_A}, \quad S_1 = \frac{d_2}{d_1}$$
$$k_1 = \frac{k_c a_0^2}{U_0}, \quad k_2 = \frac{k_s}{D_A a_0}\sqrt{\frac{\rho U_0}{\mu}}, \quad \delta = \frac{D_B}{D_A}. \tag{17}$$

The chemical species A and B won't be equal, in general, however we could anticipate that these will be equivalent in size. In the case, where the diffusion species coefficients D_B and D_A are equivalent, i.e., $\delta = 1$, then we have

$$g(\eta) + h(\eta) = 1. \tag{18}$$

Through Eqs. (13) and (14) we get the equation as

$$\frac{1}{S_c} g'' + f g' - k_1 g (1-g)^2 = 0, \tag{19}$$

and the boundary condition on concentration profile becomes

$$g'(\eta) = k_2 g(\eta), \quad \eta \to 0, \quad g(\eta) = 1, \quad \eta \to \infty. \tag{20}$$

The physically representation of the problem are shown in (Fig. 1).

Optimal homotopy analysis method

For Optimal HAM solution the essential linear operator and their initial guesses, are

$$\mathcal{L}_f(f) = \frac{d^3 f}{d\eta^3} - \frac{df}{d\eta}, \quad \mathcal{L}_\theta(\theta) = \frac{d^2\theta}{d\eta^2} - \theta, \quad \mathcal{L}_g(g) = \frac{d^2 g}{d\eta^2} - g, \tag{21}$$

$$f_0(\eta) = 1 - \exp(-\eta), \tag{22}$$
$$\theta_0(\eta) = (1 - S_1)\exp(-\eta), \tag{23}$$
$$g_0(\eta) = 1 - \frac{k_2}{1+k_2}\exp(-\eta). \tag{24}$$

Here $\mathcal{L}_f(f), \mathcal{L}_\theta(\theta)$ and $\mathcal{L}_g(g)$ are the linear operators, whereas $f_0(\eta), \theta_0(\eta)$ and $g_0(\eta)$ respectively indicate the initial approximation of f, θ and g.

Convergence through optimal homotopy analysis method

The auxiliary parameter h_f, h_θ, and h_g have incredible aim to settle and control the convergence of homotopic solutions. To obtain convergence solution we chose significant values of these parameters. For this reason, residual error are deliberated for momentum, energy and concentration expressions by utilizing the equations given below

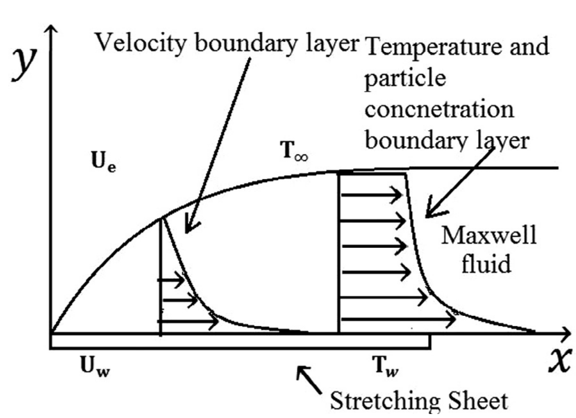

Fig. 1. Geometry of the problem.

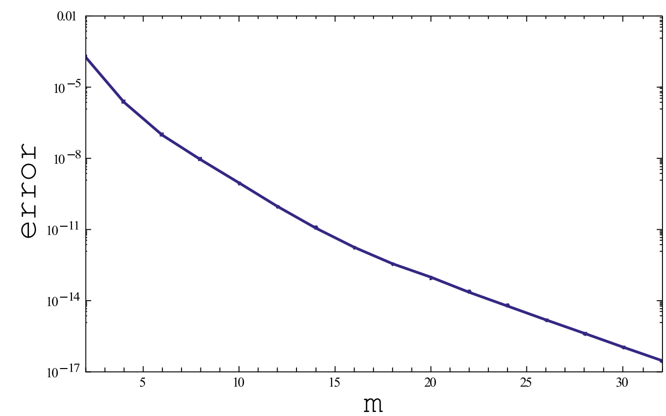

Fig. 2. Graph for 8^{th} order approximations.

$$\Delta_m^f = \int_0^1 [R_m^f(\eta, h_f)]^2 d\eta, \tag{25}$$

$$\Delta_m^\theta = \int_0^1 [R_m^\theta(\eta, h_\theta)]^2 d\eta, \tag{26}$$

$$\Delta_m^g = \int_0^1 [R_m^g(\eta, h_g)]^2 d\eta. \tag{27}$$

The convergence of the parametric values are appeared by optimal HAM, listen in the below table using the values of the parameters $k_1 = 0.8, k_2 = 0.1, S_c = 0.5, \Pr = 2.0, \delta m = 0.5, \delta e = 0.1, S_1 = 0.1$ (see Figs. 2 and 3).

Graphical illustration for the 8th and 10th order approximation are given in the following figures (Tables 1 and 2).

Here ϵ_m^t is the total discrete squared residual error.

$$\epsilon_m^t = \epsilon_m^f + \epsilon_m^\theta + \epsilon_m^g.$$

The value of ϵ_m^t is utilized to get the optimal convergence control parameters.

Results and discussion

The optimal HAM technique are used to achieve the analytical solutions for the boundary value problem. This section has been manufactured to examine the property of several physical parameters on velocity, temperature and concentration fields. The effect of dimensionless relaxation parameter δm (velocity), δe (temperature), Pr (Prandtl number), S_1 (thermal stratification), S_c (Schmidt number), k_1 (homogenous reaction) and k_2 (heterogenous reaction) are scrutinized.

Effect of δm (fluid relaxation parameter)

The influence of non-dimensionalize fluid relaxation time parameter δm on velocity profile is exhibited in Fig. 4. An increment in δm might be viewed as increment in fluid viscosity. The increased viscosity resists the fluid motion and subsequently the velocity diminishes. It is also demonstrated that the velocity boundary layer thickness reduces with an increase in δm.

Fig. 5 characterized the effects of δm on temperature field. It is found that the stronger viscous force related with the bigger δm opposes the flow and increases the temperature. This leads to the conclusion that the viscous fluid requires lower temperature than in viscoelastic fluid. Fig. 6 expressed the effect of δm on concentration profile. The concentration profile decreases with an increase in

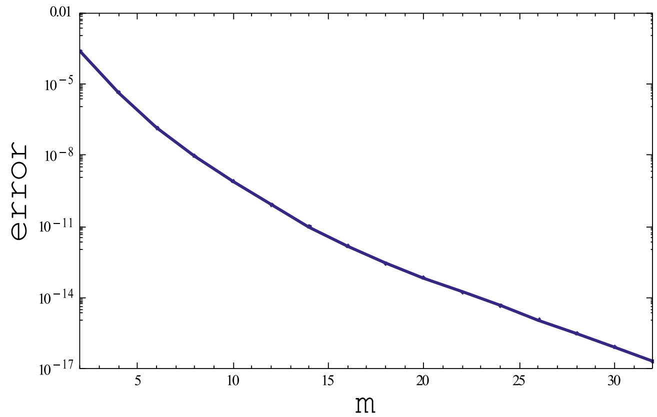

Fig. 3. Graph for 10^{th} order approximations.

δm. The value relegated to residual parameters are $\delta e = 0.1, \Pr = 2.0, S_1 = 0.1, S_c = 0.5, k_1 = 0.8$ and $k_2 = 0.1$.

Influence of δe (thermal relaxation parameter)

Fig. 7 determines the effects of thermal relaxation parameter δe on the temperature distribution and thermal boundary layer. It is noticed that the temperature field and thermal boundary layer thickness decreases for larger values of δe. This is because of certainty that as we enhances the thermal relaxation parameter, in a material the heat transfers from one particle to another particle in a slowly way. Therefore a material demonstrate a non-conducting behavior which is responsible in diminishment of temperature distribution. Further, if $\delta e = 0$ the heat transfers immediately all through the material. So for $\delta e = 0$ the temperature distribution is higher i.e., in the event of Fourier's law when compared with Cattaneo–Christov heat flux model. The value appointed to remaining parameters are $\delta m = 0.5, \Pr = 2.0, S_1 = 0.1, S_c = 0.5, k_1 = 0.8$ and $k_2 = 0.1$.

The impact of Pr *(Prandtl number)*

Fig. 8 depicts the behavior of Prandtl number on temperature field. It is described that the temperature profile and thermal boundary layer thickness diminishes with increment in Pr (Prandtl number). Physically, the thermal diffusivity decreases with enlarging the Prandtl number Pr, which comes about in the lessening of temperature profile. Further, the thermal boundary layer becomes thinner and heat diffuses gradually for bigger Pr number as compared to low Prandtl number Pr. Low Pr brings about a thicker thermal boundary layer which diffuses heat rapidly than the larger Pr. The value dispensed to closing parameters are $\delta e = 0.1, \delta m = 0.5, S_1 = 0.1, S_c = 0.5, k_1 = 0.8$ and $k_2 = 0.1$.

Table 2
Shows individual residual square errors for $\epsilon_m^f, \epsilon_m^\theta$ and ϵ_m^g.

values→ order↓	$h_f = -0.796684$	$h_\theta = -1.37584$	$h_g = -1.59953$
	ϵ_m^f	ϵ_m^θ	ϵ_m^g
4	2.91014×10^{-7}	3.4555×10^{-6}	4.33396×10^{-7}
8	7.90562×10^{-10}	4.59122×10^{-9}	4.15131×10^{-9}
12	2.60818×10^{-15}	1.03716×10^{-15}	9.68335×10^{-16}
20	3.35617×10^{-18}	1.06608×10^{-18}	1.15095×10^{-18}

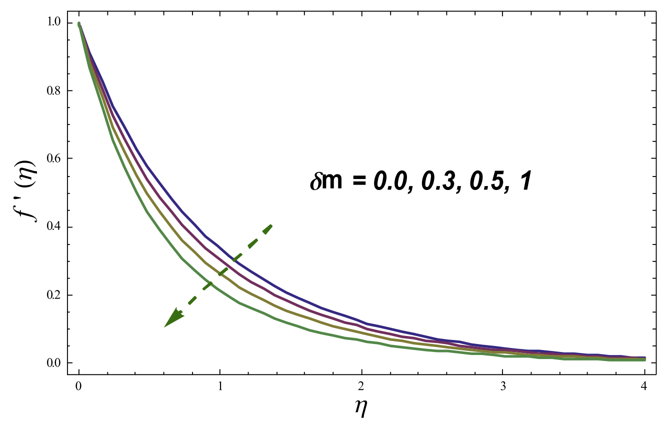

Fig. 4. Effect of δm on $f'(\eta)$.

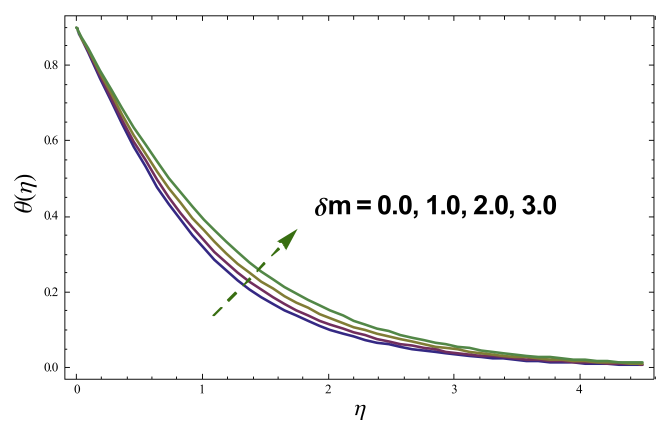

Fig. 5. Effect of δm on $\theta(\eta)$.

The effects of parameters S_1 (thermal stratification) and S_c (Schmidt number)

Fig. 9 demonstrates the variety of temperature profile because of an adjustment in the values of thermal stratification parameter

Table 1
For average residual square errors (ϵ_m^t).

values→ order↓	h_f	h_θ	h_g	ϵ_m^t
2	−0.818921	−1.14615	−1.58336	0.0000620295
4	−0.770922	−1.20039	−1.59727	7.89411×10^{-7}
6	−0.759381	−1.27857	−1.60033	7.64902×10^{-8}
8	−0.787575	−1.34167	−1.60057	8.81702×10^{-9}
10	−0.796684	−1.37584	−1.59953	8.08651×10^{-10}

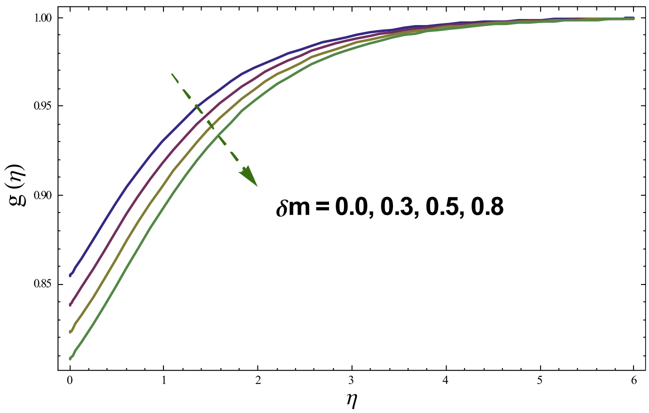

Fig. 6. Effect of δm on $g(\eta)$.

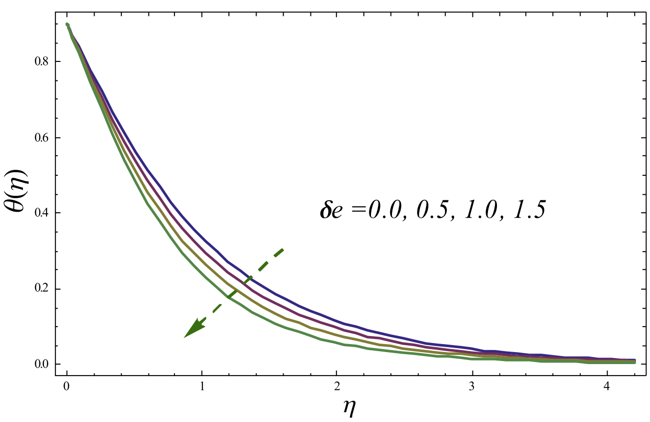

Fig. 7. Effect of δe on $\theta(\eta)$.

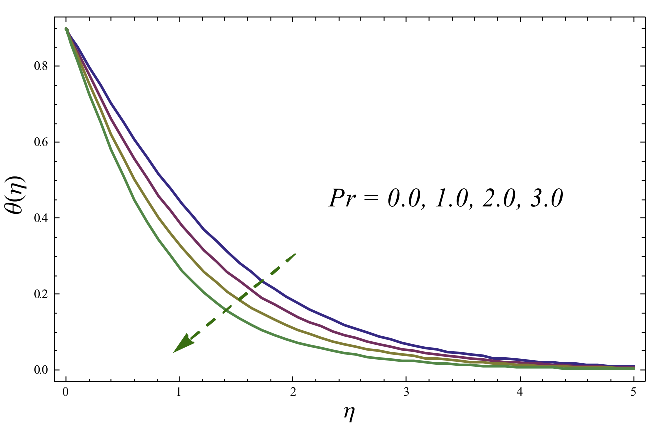

Fig. 8. Effect of Pr on $\theta(\eta)$.

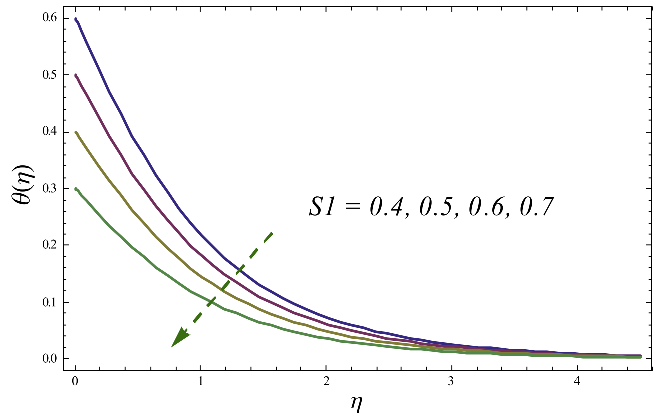

Fig. 9. Effect of S_1 on $\theta(\eta)$.

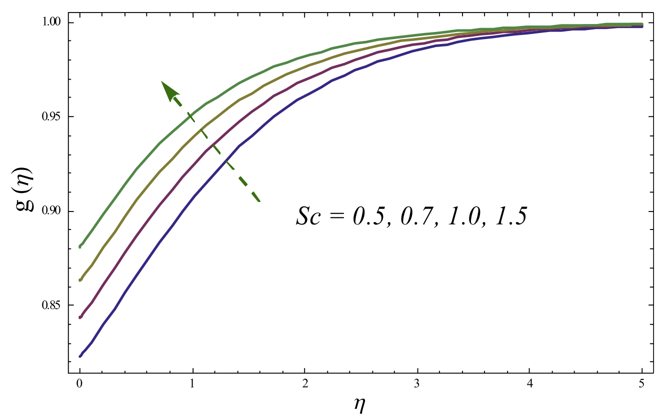

Fig. 10. Effect of S_c on $g(\eta)$.

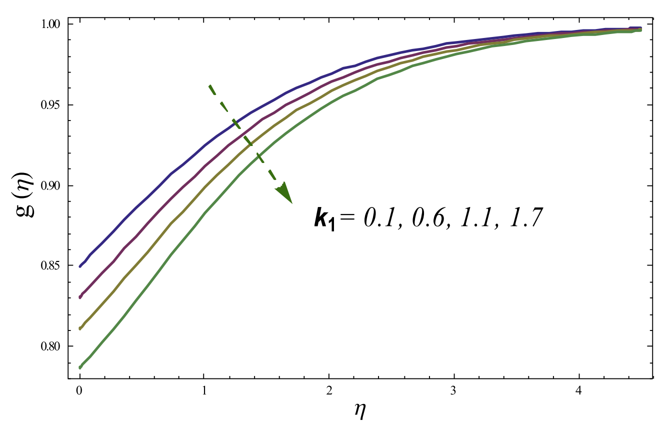

Fig. 11. Effect of k_1 on $g(\eta)$.

S_1. It is observed that the temperature field diminishes with an increase in the values of S_1. Further, the thermal boundary layer thickness also diminishes with increment in S_1. This is due to the temperature differences reasonably decays amongst surface and ambient of sheet.

Fig. 10 signifies the influence of S_c (Schmidt number) on concentration field. Schmidt number S_c is the proportion between the momentum diffusivity and mass diffusivity. Because of this S_c is inversely proportional to mass diffusivity the boundary layer thickness decrease and concentration field enhances. The value gives to remaining parameters are $\delta m = 0.5, \delta e = 0.1, \mathrm{Pr} = 2.0$, $k_1 = 0.8$ and $k_2 = 0.1$.

Effects of parameters k_1 and k_2 (strength of homogeneous and heterogeneous reaction)

In this subsection we study the impact of parameters k_1 (homogeneous reaction) and k_2 (heterogeneous reaction) on concentration field. Fig. 11 review the impact of homogeneous reaction k_1 on concentration distribution $g(\eta)$. It is found that concentration

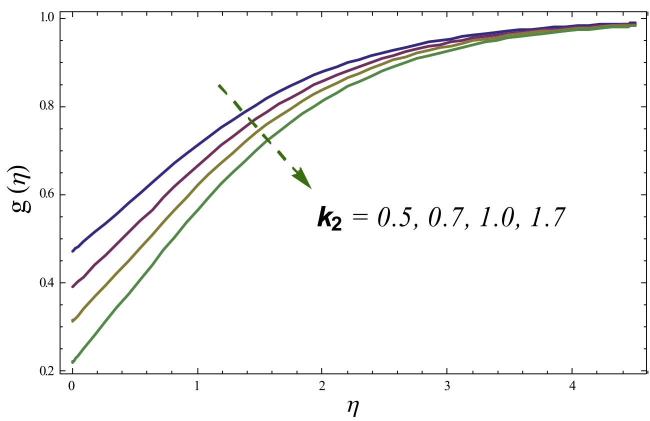

Fig. 12. Effect of k_2 on $g(\eta)$.

distribution diminishes with enhancement in the values of k_1. Moreover the effect of heterogeneous reaction parameter k_2 on concentration field is indicated in Fig. 12. The reduction is occur in concentration field with enlarging the values of k_2 because heterogeneous reaction parameter k_2 has reverse convection with mass diffusivity. The values allocated to closing parameters are $\delta e = 0.1, \delta m = 0.5, \Pr = 2.0, S_1 = 0.1$ and $S_c = 0.5$.

Concluding remarks

The properties of the homogeneous-heterogeneous reaction in a two-dimensional Maxwell fluid is carried out in the present of thermal stratification. The Cattaneo–Christov heat flux model is used instead of Fourier's law of heat conduction. The optimal HAM are used to got the analytical series solutions of the boundary value problem. The conclusion drawn from the flow analysis are the following.

(i) The velocity boundary layer thickness and concentration profile have inverse behavior with fluid relaxation parameter δm. While temperature field increases with the increase of relaxation time δm.
(ii) Temperature distribution is higher for Fourier's law than Cattaneo-Cristov heat flux model.
(iii) Thermal boundary layer thickness increases with the increases of Prandtl number Pr.
(iv) Temperature profile shows increasing behavior for large values of S_1.
(v) The effect of Schmidt number S_c on concentration distribution is increasing.
(vi) The influence of the strength of homogeneous and heterogeneous reaction on concentration field is diminishes.

Acknowledgment

Authors would like to acknowledge and express their gratitude to the Qatar University, Doha, Qatar for providing the financial support to publish this aritcle.

References

[1] Crane LJ. Flow past a stretching plate. Zeitschrift für angewandte Mathematik und Physik ZAMP 1970;21(4):645–7.
[2] Dutta BK, Roy P, Gupta AS. Temperature field in flow over a stretching sheet with uniform heat flux. Int Commun Heat Mass Transfer 1985;12(1):89–94.
[3] Char MI. Heat transfer of a continuous, stretching surface with suction or blowing. J Math Anal Appl 1988;135(2):568–80.
[4] Gupta PS, Gupta AS. Heat and mass transfer on a stretching sheet with suction or blowing. Can J Chem Eng 1977;55(6):744–6.
[5] Nadeem S, Haq RU, Khan ZH. Heat transfer analysis of water-based nanofluid over an exponentially stretching sheet. Alexandria Eng J 2014;53(1):219–24.
[6] Mukhopadhya S. Slip effects on MHD boundary layer flow over an exponentially stretching sheet with suction/blowing and thermal radiation. Ain Shams Eng J 2013;4(3):485–91.
[7] Zhang Y, Zhang M, Bai Y. Unsteady flow and heat transfer of power-law nanofluid thin film over a stretching sheet with variable magnetic field and power-law velocity slip effect. J Taiwan Inst Chem Eng 2017;70:104–10.
[8] Majeed A, Zeeshan A, Ellahi R. Unsteady ferromagnetic liquid flow and heat transfer analysis over a stretching sheet with the effect of dipole and prescribed heat flux. J Mol Liq 2016;223:528–33.
[9] Pal D, Saha P. Influence of nonlinear thermal radiation and variable viscosity on hydromagnetic heat and mass transfer in a thin liquid film over an unsteady stretching surface. Int J Mech Sci 2016;119:208–16.
[10] Weidman P, Turner MR. Stagnation-point flows with stretching surfaces: a unified formulation and new results. Eur J Mech B Fluids 2017;61:144–53.
[11] Fourier J. Theorie analytique de la chaleur, Par M. Fourier. Chez Firmin Didot, père et fils, 1822.
[12] Carlo Cattaneo. Sulla conduzione del calore. In: In some aspects of diffusion theory. Berlin Heidelberg: Springer; 2011. 485–485.
[13] Christov CI. On frame indifferent formulation of the Maxwell-Cattaneo model of finite-speed heat conduction. Mech Res Commun 2009;36(4):481–6.
[14] Nadeem S, Muhammad N. Impact of stratification and Cattaneo–Christov heat flux in the flow saturated with porous medium. J Mol Liq 2016;224:423–30.
[15] Khan M. On Cattaneo–Christov heat flux model for Carreau fluid flow over a slendering sheet. Results Phys 2016.
[16] Abbasi FM, Shehzad SA. Heat transfer analysis for three-dimensional flow of Maxwell fluid with temperature dependent thermal conductivity: application of Cattaneo–Christov heat flux model. J Mol Liq 2016;220:848–54.
[17] Ramzan M, Bilal M, Chung JD. Effects of MHD homogeneous-heterogeneous reactions on third grade fluid flow with Cattaneo–Christov heat flux. J Mol Liq 2016;223:1284–90.
[18] Khan M, Khan WA. Three-dimensional flow and heat transfer to burgers fluid using Cattaneo–Christov heat flux model. J Mol Liq 2016;221:651–7.
[19] Muhammad N, Nadeem S, Mustafa T. Squeezed flow of a nanofluid with Cattaneo–Christov heat and mass fluxes. Results Phys 2017.
[20] Jamil M, Fetecau C. Helical flows of Maxwell fluid between coaxial cylinders with given shear stresses on the boundary. Nonlinear Anal Real World Appl 2010;11(5):4302–11.
[21] Awasthi MK, Kumar V, Patel RK. Onset of triply diffusive convection in a Maxwell fluid saturated porous layer with internal heat source. Ain Shams Eng J 2016.
[22] Ramesh GK, Gireesha BJ, Hayat T, Alsaedi A. Stagnation point flow of Maxwell fluid towards a permeable surface in the presence of nanoparticles. Alexandria Eng J 2016;55(2):857–65.
[23] Zhao J, Zheng L, Zhang X, Liu F. Unsteady natural convection boundary layer heat transfer of fractional Maxwell viscoelastic fluid over a vertical plate. Int J Heat Mass Transfer 2016;97:760–6.
[24] Li C, Zheng L, Zhang X, Chen G. Flow and heat transfer of a generalized Maxwell fluid with modified fractional Fourier's law and Darcy's law. Comput Fluids 2016;125:25–38.
[25] Chaudhary MH, Merkin JH. A simple isothermal model for homogeneous-heterogeneous reactions in boundary-layer flow. II Different diffusivities for reactant and autocatalyst. Fluid Dyn Res 1995;16(6):335.
[26] Chaudhary MA, Merkin JH. A simple isothermal model for homogeneous-heterogeneous reactions in boundary-layer flow. I Equal diffusivities. Fluid Dyn Res 1995;16(6):311–33.
[27] Merkin JH. A model for isothermal homogeneous-heterogeneous reactions in boundary-layer flow. Math Comput Modell 1996;24(8):125–36.
[28] Nadeem S, Ahmad Shafiq, Muhammad Noor. Cattaneo–Christov flux in the flow of a viscoelastic fluid in presence of Newtonian heating. J Mol Liq 2017.
[29] Muhammad N, Nadeem Sohail, Haq RU. Heat transport phenomenon in the ferromagnetic fluid over a stretching sheet with thermal stratification. Results Phys 2017;7:854–61.
[30] Nawaz M, Zeeshan A, Ellahi R, Abbasbandy S, Rashidi Saman. Joules and Newtonian heating effects on stagnation point flow over a stretching surface by means of genetic algorithm and Nelder-Mead method. Int J Numer Methods Heat Fluid Flow 2015;25(3):665–84.
[31] Zeeshan A, Majeed A, Ellahi R. Effect of magnetic dipole on viscous ferro-fluid past a stretching surface with thermal radiation. J Mol Liq 2016;215:549–54.
[32] Majeed A, Zeeshan A, Ellahi R. Unsteady ferromagnetic liquid flow and heat transfer analysis over a stretching sheet with the effect of dipole and prescribed heat flux. J Mol Liq 2016;223:528–33.
[33] Maqbool K, Sohail A, Manzoor N, Ellahi R. Hall effect on Falkner—Skan boundary layer flow of FENE-P fluid over a stretching sheet. Commun Theor Phys 2016;66(5):547.
[34] Sheikholeslami M, Ganji DD, Javed MY, Ellahi R. Effect of thermal radiation on magnetohydrodynamics nanofluid flow and heat transfer by means of two phase model. J Magn Magn Mater 2015;374:36–43.
[35] Sheikholeslami M, Ellahi R. Electrohydrodynamic nanofluid hydrothermal treatment in an enclosure with sinusoidal upper wall. Appl Sci 2015;5(3):294–306.
[36] Zeeshan A, Majeed A, Ellahi R. Effect of magnetic dipole on viscous ferro-fluid past a stretching surface with thermal radiation. J Mol Liq 2016;215:549–54.

[37] Akbarzadeh M, Rashidi S, Bovand M, Ellahi R. A sensitivity analysis on thermal and pumping power for the flow of nanofluid inside a wavy channel. J Mol Liq 2016;220:1–13.
[38] Bhatti MM, Zeeshan A, Ellahi R. Study of heat transfer with nonlinear thermal radiation on sinusoidal motion of magnetic solid particles in a dusty fluid. J Theor Appl Mech 2016;46(3):75–94.
[39] Shirvan KM, Ellahi Rahmat, Mirzakhanlari S, Mamourian M. Enhancement of heat transfer and heat exchanger effectiveness in a double pipe heat exchanger filled with porous media: numerical simulation and sensitivity analysis of turbulent fluid flow. Appl Therm Eng 2016;109:761–74.